Indentation Response and Contact Damage of Hard T-B-N Films Deposited by Magnetron Sputtering

P. Karuna Purnapu Rupa[1], P. C. Chakraborti[2], Suman.K.Mishra[3]

[1] Non Ferrous Materials Technology Development Centre, PO Kanchanbagh, Hyderabad 500058, India
[2] Department of Metallurgy and Materials Engineering, Jadavpur University, Kolkata 700032, India
[3] National Metallurgical Laboratory, Jamshedpur 831007, India

Abstract

Titanium-boron-nitride (Ti-B-N) films were deposited by reactive magnetron sputtering using a single TiB2 target. The films were deposited under different Ar:N_2 ratios. The instrumented indentation technique (nanoindentation), is used to evaluate the mechanical properties of the films. A methodology is presented to evaluate the critical load to failure directly from the load depth curves. Significant effect of Ar:N2 ratio was observed on the mechanical properties of the Ti-B-N films.

Introduction

Recently there has been lot of interest in the nanocomposite thin films based on Titanium-Boron-Nitrogen (Ti-B-N) system. The nanocomposite thin films have good mechanical properties and exhibit excellent chemical and thermal stability [1-6]. This is due to the formation of hard phases such as Titanium diboride (TiB_2), Titanium nitride (TiN) and soft phase such as hexagonal-BN within the ternary Ti-B-N phase diagram [7]. One of the ways of obtaining Ti-B-N films is through magnetron sputtering using TiB_2 target and nitrogen as a reactive gas. TiB_2 films exhibit compressive stress during the film growth and have low fracture toughness [8, 9]. The nitrogen incorporation in the TiB2 films is expected to increase the toughness.

The mechanical properties of the films are evaluated using nanoindentation. This technique has a low depth and load resolution. The load (P) and the depth (h) during indentation is continuously measured. The hardness and modulus are then extracted. Hard films upon indentation exhibit different failure modes such as radial cracks, circumferential cracks etc which are dependent on the substrate and the film properties [9].

In this paper the indentation response of the Ti-B-N films deposited by magnetron sputtering using a single TiB_2 target in Ar-N_2 gas mixtures is investigated. A methodology is presented wherein the critical load for failure of the films can be evaluated directly from the P-h curves obtained from nanoindentation.

Experimental

The Ti-B-N films were deposited by magnetron sputtering using a single TiB_2 target with different Ar-N_2 gas ratios. The deposition conditions are shown in Table 1. After the deposition (Nanoindentation Nanoindenter XP) was performed on the films using a Berkovich indenter to determine elastic modulus and hardness. The properties were evaluated using the Oliver and Pharr's analysis technique [10]. The instrument was operated in the continuous stiffness mode (CSM) and the indentations were made using a constant nominal strain rate of 0.05 s–1 and a frequency of 45 Hz. The harmonic displacement was 3 nm. Poisson's ratio of 0.25 was used to calculate the elastic modulus.

Nanoindentation hardness is defined as projected contact area of the indentation. From the load–displacement curve, hardness can be obtained at the peak load as

$$H = P_{max} / A \qquad (1)$$

where, A is the projected contact area.

*corresponding author. E-mail: pkprupa@gmail.com

© 2011 al-Farabi Kazakh National University Printed in Kazakhstan

Using relations developed by Sneddon [11] the contact area in turn may be related to the measured contact stiffness, S, by

$$S = 2\beta\ Er\ (A/\pi)^{1/2} \qquad (2)$$

where, β is a constant that depends on the geometry of the indenter (β = 1.034 for a Berkovich indenter) and Er is the reduced elastic modulus given by

$$1/E_r = (1 - \nu^2)/E + (1 - \nu_i^2)/E_i \qquad (3)$$

where, E and ν are the elastic modulus and Poisson's ratio for the film respectively, and E_i and νi are the same quantities for the indenter. For diamond, E_i = 1141 GPa and νi = 0.07 and S = (dP/dh)h=hmax, h is the displacement of the indenter into surface.

Table 1.
The deposition conditions

Deposition pressure(Pa)	Ar:N_2 ratio	N_2 fraction		
			Tempe-rature	500°C
1	100:0	0	Power	120W
1.5	99.34:0.66	0.006		
1	99:1	0.01	Deposition time	90 minutes
1.5	7:93	0.93		

Results and discussion

Figure 1, shows the load vs. displacement (P-h) curve of indentation on TiB_2 film on silicon substrate. The curve is very smooth during loading. During unloading a kink is observed which is due to the load induced phase transformation of the silicon. To analyse the P-h curves of TiB_2-Si further the slope of the loading curve vs. displacement is plotted (Fig. 2). Several marked discontinuities are observed as shown by the arrows. The first discontinuity occurs at a depth of 265 nm. Thus, we can observe that these discontinuities are revealed more easily from the slope of the P-h curve than the P-h curves itself. It has been established that these correspond to the fracture or failure events of the thin films where the first kink corresponds to the onset of radial cracking of the films [9]. This also corresponds to the critical load for fracture. For the TiB_2 film, from the P-h curve, this corresponds to a critical load of 30 mN.

The nitrogen incorporation in the TiB_2 films is expected to have bearing on the critical load to fracture. This is due to the formation of nanocomposite nature with two crystalline phases or a composite of a crystalline and an amorphous phase. The slope of the Ti-B-N films deposited on silicon substrates with different Ar-N_2 ratios (N_2 fraction) is shown in Figure-3 a,b,c,d. It can be observed from the slope of the P-h curves (figure-3b) that a kink in the loading curve of the film deposited at N_2 fraction of 0.006 is observed at 536 nm which corresponds

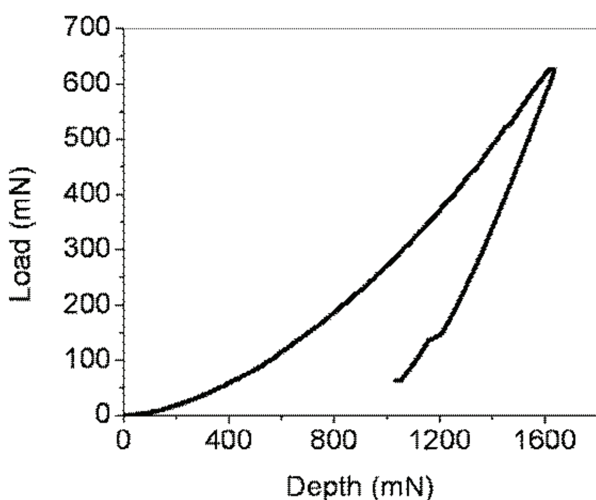

Fig. 1. Load vs. depth (P-h) curve of TiB_2 film on silicon substrate

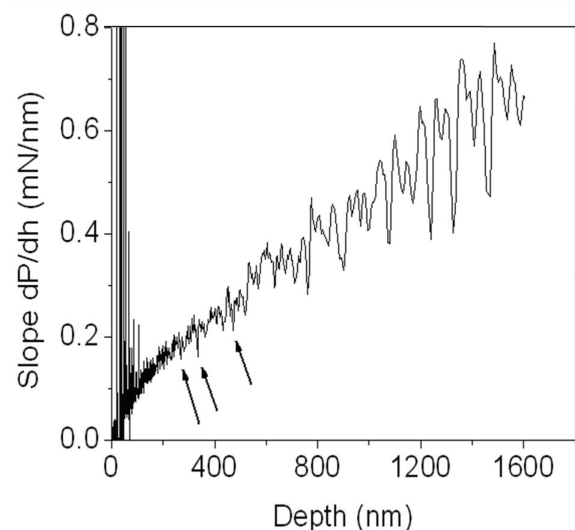

Fig. 2. Slope of the loading curve (dP/dh) vs. depth of TiB_2 film on silicon substrate

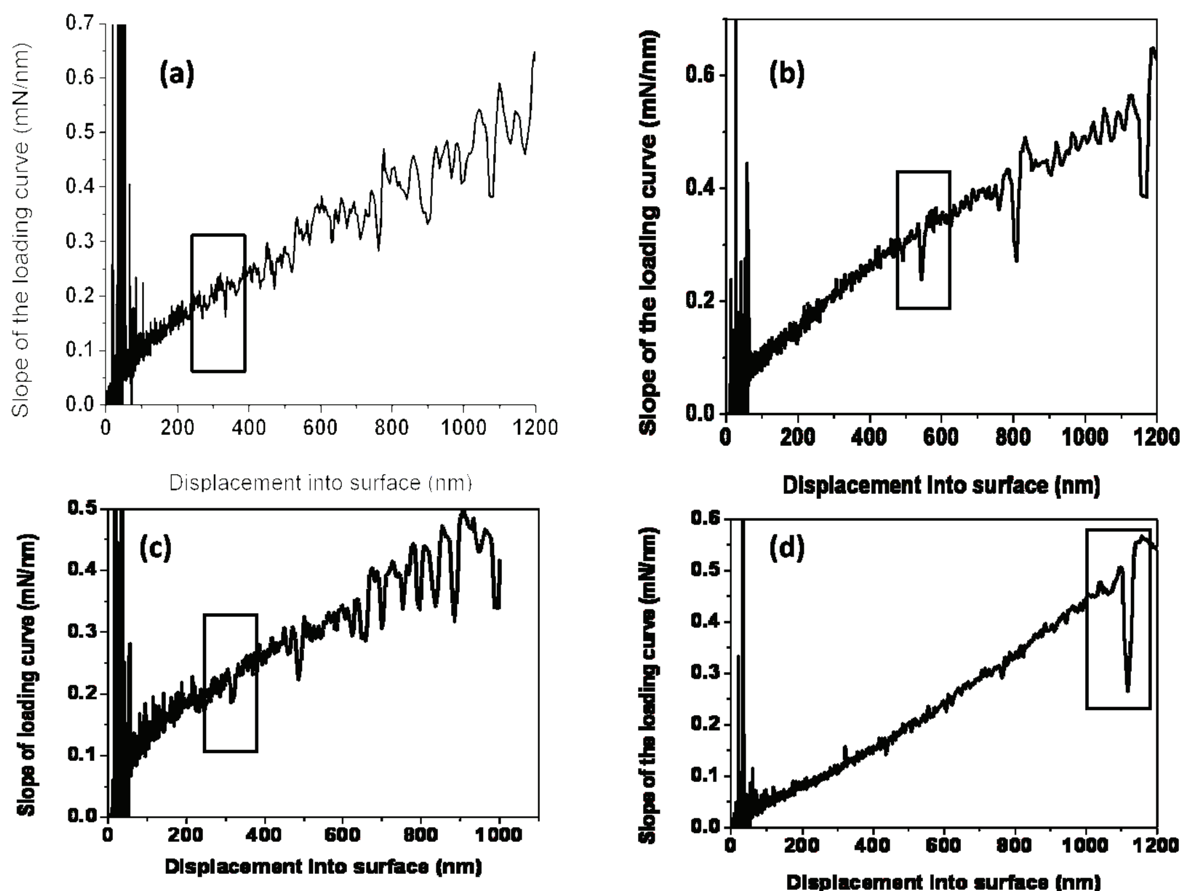

Fig. 3. Slope of the loading curve vs. depth for films (a) TiB_2, (b) N_2 fraction of 0.006, (c) N_2 fraction of 0.01 and (d) N_2 fraction of 0.93. The fracture events are shown in the box.

to a load of 100 mN. As the N_2 fraction increases (0.01), the first kink is observed an indentation depth of 309 nm at a load of 45 mN (figure-3c). This shows that the film deposited at N_2 fraction of 0.006 exhibits a higher critical load for fracture than for the film deposited at N_2 fraction of 0.01 and TiB_2. For the film deposited at high N_2 fraction of 0.93, the kink is observed at 1117nm indentation depth which corresponds to a load of 256 mN (figure 3d). Thus the film deposited at high N_2 fraction exhibits very high critical load for failure. Many researchers have reported the formation of hexagonal – boron nitride (h-BN) at high N_2 fractions [12, 13]. The soft h-BN thus plays a role in enhancing the critical load. But for optimum properties the critical load for failure has to match with good hardness. Figure 4, shows the plot of critical load for failure vs. hardness of the Ti-B-N films determined by nanoindentation. It can be observed that with the decrease in the hardness the critical load increases. This clearly shows that the nitrogen incorporation in the films is playing a role and the relative mole fraction of h-BN in the film is influencing the mechanical properties of the Ti-B-N films.

Conclusions

Ti-B-N films were successfully deposited using DC magnetron sputtering. The hardness of the films varied from 42 GPa for TiB_2 films to 6 GPa for films deposited under high nitrogen fraction. Analysis of the slope of the load depth curve obtained from nanoindentation has shown several kinks or discontinuities which correspond to the critical load for failure. Significant effect of the nitrogen fraction was observed on the critical load. The critical load decreased with increase in the N_2 fraction.

References

1. Wiedemann, R., Weihnacht. V., and Oettel, H., Surf. Coat. Technol. 116–119: 302 (1999).
2. García-Luis. A., Brizuela. M., Oñate, J.I., Sánchez-López, J.C., Martínez-Martínez, D.,

López-Cartes, C., and Fernández, A., Surf. Coat. Technol. 200: 734 (2005).
3. Lu, Y.H., Shen, Y.G., Zhou, Z.F., and Li, K.Y., J. Vac. Sci.Technol. A 24: 340 (2006).
4. Mayrhofer, P.H., Mitterer, C., Wen, J.G., Petrov, I., Greene, J.E., J. Appl. Phys. 100: 044301 (2006)
5. Musil, J., Surf. Coat. Technol. 125: 322 (2000).
6. Karvankova, P., Veprek-Heijman, M.G.J., Zindulka, O., Bergmaier, A., and Veprek, S., Surf. Coat. Technol. 163–164: 149 (2003).
7. Novotny, H., Benesovsky, F., Brukl, C., and Schob, O., Mh. Chem. 92: 403 (1961).
8. Berger, M., Coronel, E., and Olsson, E., Surf. Coat. Technol. 185: 240 (2004).
9. Rupa, P. K. P., Chakraborti P. C., and Mishra, S. K., Thin Solid Films. 517: 2912 (2009).
10. Oliver, W.C., Pharr, G.M., J. Mater. Res. 7: 1564 (1992).
11. Sneddon, I. N., Int. J. Eng. Sci. 3: 47 (1965).
12. López-Cartes, C., Martínez-Martínez, D., Sánchez-López, J. C., Fernández, A., García-Luis, A., Brizuela, M., and Oñate, J. I., Thin Solid Films. 515: 3590 (2007).
13. Héau, C., and Terrat, J. P., Surf.Coat.Technol. 108-109: 332. (1998).

Received 16 June 2010.